

1 **Recapitulation of SARS-CoV-2 Infection and** 2 **Cholangiocyte Damage with Human Liver Organoids**

3

4 **Bing Zhao^{1,6,*}, Chao Ni^{1,6}, Ran Gao^{2,6}, Yuyan Wang³, Li Yang¹, Jinsong Wei¹, Ting Lv⁴,**
5 **Jianqing Liang¹, Qisheng Zhang⁵, Wei Xu³, Youhua Xie³, Xiaoyue Wang², Zhenghong**
6 **Yuan³, Junbo Liang^{2,*}, Rong Zhang^{3,*} and Xinhua Lin^{1,*}**

7

8 ¹State Key Laboratory of Genetic Engineering, School of Life Sciences, Zhongshan
9 Hospital, Fudan University, Shanghai 200438, China; ²State Key Laboratory of Medical
10 Molecular Biology, Institute of Basic Medical Sciences, Chinese Academy of Medical
11 Sciences, Peking Union Medical College, Beijing 100005, China; ³Key Laboratory of
12 Medical Molecular Virology (MOE/NHC/CAMS), School of Basic Medical Sciences,
13 Shanghai Medical College, Fudan University, Shanghai 200032, China; ⁴Institute of
14 Antibiotics, Huashan Hospital, Fudan University, Shanghai 200040, China; ⁵Sino
15 Organoid Lifesciences Ltd., Shanghai 201900, China; ⁶These authors contributed
16 equally to this work.

17

18 *Correspondence and requests for materials should be addressed to B.Z.
19 (bingzhao@fudan.edu.cn), J.L. (liangjunbo@ibms.pumc.edu.cn), R.Z.
20 (rong_zhang@fudan.edu.cn) or X.L. (xlin@fudan.edu.cn).

21

22

23

24 Short title: The novel coronavirus injures cholangiocytes

25

26 Keywords: SARS-CoV-2; human liver organoids; ACE2+ cholangiocytes; liver damage

27

28 The newly emerged pandemic coronavirus, SARS-CoV-2, has posed a significant
29 public health threat worldwide. However, the mode of virus transmission and
30 tissue tropism is not well established yet. Recent findings of substantial liver
31 damage in patients and ACE2+ cholangiocytes in healthy liver tissues prompted us
32 to hypothesize that human liver ductal organoids could serve as a model to
33 determine the susceptibility and mechanisms underlining the liver damage upon
34 SARS-CoV-2 infection. By single-cell RNA sequencing, we found that long-term liver
35 ductal organoid culture preserved the human specific ACE2+ population of
36 cholangiocytes. Moreover, human liver ductal organoids were permissive to
37 SARS-CoV-2 infection and support robust replication. Notably, virus infection
38 impaired the barrier and bile acid transporting functions of cholangiocytes through
39 dysregulation of genes involved in tight junction formation and bile acid
40 transportation, which could explain the bile acid accumulation and consequent
41 liver damage in patients. These results indicate that control of liver damage caused
42 directly by viral infection should be valued in treating COVID-19 patients. Our
43 findings also provide an application of human organoids in investigating the
44 tropism and pathogenesis of SARS-CoV-2, which would facilitate novel drug
45 discovery.

46 **Introduction**

47 A recent outbreak of SARS-CoV-2 (previously named 2019-nCoV) infection in
48 Wuhan (China) has caused emergent and significant threats to global public health¹.
49 The dominant symptoms of coronavirus disease 2019 (COVID-19) are fever and
50 cough^{2,3}. However, a proportion of patients showed multi-organ damage and
51 dysfunction²⁻⁴. Of note, liver damage is emerging as a co-existed symptom reported
52 in patients with COVID-19. A recent epidemiologic study in Shanghai (China)
53 reported that 75 out of 148 (50.7%) COVID-19 patients had liver function
54 abnormality, indicated by key liver function parameters above the normal range,
55 including alanine aminotransferase (ALT), aspartate aminotransferase (AST), alkaline
56 phosphatase (ALP) or total bilirubin (TBIL)⁵. A national wide clinical study collecting
57 1,099 COVID-19 patients revealed that around 20% of patients had elevated ALT and
58 AST and around 10% of patients had elevated TBIL. Especially, the percentage of
59 patients with liver damage is much higher in severe patients than that in non-severe
60 ones². Although the clinical correlation has been implicated, it is still unclear whether
61 the liver damage is caused by direct virus infection in the liver or by systematic
62 reasons such as cytokine storm.

63 Viruses bind to host receptors to initiate the infection. Recent studies have
64 demonstrated that both SARS-CoV-2 and SARS-CoV use the same
65 angiotensin-converting enzyme 2 (ACE2) protein to enter the cells⁶⁻¹⁰. It has been
66 shown that ACE2 expression is widely distributed across human tissues, including
67 lung, liver, kidney and multiple digestive tract organs¹¹⁻¹³. A significant enrichment of

68 ACE2+ population in cholangiocytes compared to hepatocytes in human healthy liver
69 was reported recently¹⁴, implying that SARS-CoV-2 might directly target ACE2+
70 cholangiocytes in patients. However, whether the virus indeed infects human
71 cholangiocytes thus causes local damage has not been addressed yet.

72 At present, due to the lack of suitable research models, studies on mechanisms of
73 SARS-CoV-2 pathogenesis mainly depend on bioinformatics analysis, clinical
74 characteristics and rare autopsy reports¹⁵. Here we report the use of human
75 organoids as a tool to investigate the SARS-CoV-2 infection and induced tissue
76 damage ex vivo at the cellular and molecular levels. By single-cell RNA sequencing,
77 we found that long-term human liver ductal organoid culture preserved the human
78 specific ACE2+ population of cholangiocytes. Moreover, human liver ductal
79 organoids were susceptible to SARS-CoV-2 infection and support robust viral
80 replication. Notably, virus infection impaired the barrier and bile acid transporting
81 functions of cholangiocytes in human liver ductal organoids. These results suggest
82 that the dysfunction of cholangiocytes induced by SARS-CoV-2 infection could
83 contribute to the bile acid accumulation and consequent liver damage in patients,
84 and control of liver damage should be valued in treating COVID-19 patients. Our
85 findings also provide a useful model of SARS-CoV-2 infection for pathogenesis study
86 and novel drug discovery.

87 **Results**

88 **ACE2+ cholangiocytes are preserved in human liver ductal organoid cultures.**

89 To establish the SARS-CoV-2 infection model with human liver ductal organoids,
90 we first determined whether the long-term organoid culture could preserve the
91 ACE2+ cholangiocytes ex vivo. We processed single-cell RNA sequencing (scRNA-seq)
92 to interrogate the transcriptome of cholangiocytes in human liver ductal organoids.
93 A total number of 7,978 cells were analyzed and cell populations were visualized by
94 t-distributed stochastic neighbor embedding (t-SNE), partitioning the cells into 7
95 clusters (Fig. 1A). The common cholangiocyte markers *EPCAM* and *KRT19* were
96 uniformly highly expressed in all the 7 clusters, indicating the heterogeneity of
97 cholangiocytes in these organoids was relatively low (Fig. 1B). Notably, we identified
98 the SARS-CoV-2 receptor gene *ACE2* expressed sparsely among cluster 0-5 in
99 unbiased preferences and was detectable in 2.92% cells (233 out of 7,978) (Fig. 1C,
100 D). Anti-ACE2 immunostaining further verified the presence of ACE2+ cholangiocytes
101 in human liver ductal organoids (Fig. 1E). Interestingly, we found that the
102 cholangiocytes in mouse primary liver ductal organoids had comparable *Epcam*
103 expression but no *Ace2* (mouse *Ace2*) expression (Fig. 1F). Taken together, our data
104 demonstrate that long-term human liver ductal organoid culture preserves the
105 human specific ACE2+ population of cholangiocytes and the human liver ductal
106 organoids could serve as a model to study the SARS-CoV-2 infection mediated by
107 receptor ACE2.

108

109 **Recapitulation of SARS-CoV-2 infection in human Liver ductal organoids.**

110 We next examined the susceptibility of human liver ductal organoids to
111 SARS-CoV-2. We isolated and plaque-purified the SARS-CoV-2 from a COVID-19
112 patient in Shanghai. The liver ductal organoids from two individuals were inoculated
113 with SARS-CoV-2 for 1 hour then re-embedded in Matrigel and maintained in culture
114 medium. We performed immunostaining to identify the virus-positive cholangiocytes
115 24 hours post infection. The expression of SARS-CoV-2 nucleocapsid protein was
116 readily detected in patchy areas of human liver ductal organoids whereas no signal
117 was found in uninfected control (Figure 2A). In addition, the infected cholangiocytes
118 underwent membrane fusion and formed syncytia (Figure 2A, enlarge). Although the
119 number of infected cholangiocytes was limited, qRT-PCR analysis of the SARS-CoV-2
120 genomic RNAs revealed a dramatic increase of viral load in organoids at 24 hours
121 post infection (Figure 2B). These data demonstrate that human liver ductal organoids
122 are susceptible to SARS-CoV-2 and support robust viral replication. The
123 recapitulation of SARS-CoV-2 infection in human organoids suggests that this model
124 could be employed to dissect the viral pathogenesis and to test antivirals.

125

126 **SARS-CoV-2 infection impairs the barrier and bile acid transporting functions of**
127 **cholangiocytes.**

128 The viral load in organoids was significantly decreased at 48 hours post infection
129 (Figure 2B), probably due to virus-induced death of host cholangiocytes or activation
130 of anti-viral response. This promoted us to detect whether SARS-CoV-2 infection
131 could influence the tissue behavior.

132 The main function of cholangiocytes in homeostasis is to transport bile acid
133 secreted by hepatocytes into bile ducts. The tight junction between cholangiocytes
134 maintains the barrier function of bile ductal epithelium, which is essential for bile
135 acid collection and excretion. We found that SARS-CoV-2 infection ablated the
136 expression of Claudin1 (Figure 3), suggesting that the barrier function of
137 cholangiocytes was disrupted. More importantly, the expression of two major bile
138 acid transporters, apical sodium-dependent bile acid transporter (ASBT) and cystic
139 fibrosis transmembrane conductance regulator (CFTR), was significantly reduced
140 following SARS-CoV-2 infection (Figure 3). These data indicate that SARS-CoV-2
141 infection impairs the barrier and bile acid transporting functions of cholangiocytes
142 through modulating the expression of genes involved in tight junction formation and
143 bile acid transportation. Our study therefore supports the idea that the liver damage
144 in COVID-19 patients might be resulted from direct cholangiocyte injury and
145 consequent bile acid accumulation induced by viral infection.

146 **Discussion and Conclusion**

147 Organoids retain the biology of individual tissues, which hold great promise for the
148 study of host–microbe interaction¹⁶. Here we demonstrated that long-term human
149 liver ductal organoid culture preserves the human specific ACE2+ population of
150 cholangiocytes. The SARS-CoV-2 exposure experiments revealed that the virus infects
151 and replicates efficiently in these organoids. To our knowledge, this is the first
152 SARS-CoV-2-human organoid infection model reported. Given that the culture
153 conditions for various organoids (lung, intestine and kidney) have been established, it
154 would be intriguing to study the tropism, replication, and innate immune response of
155 SARS-CoV-2 infection in other organs that are targeted by this virus.

156 It appears that liver dysfunction or damage in severe patients with COVID-19 is a
157 common but unignored phenomena. The improper use of anti-viral drugs may be
158 hepatotoxic and cause liver damage. On the other hand, SARS-CoV-2 infection may
159 trigger overwhelming inflammatory response and lead to tissue injury at multi-organ
160 levels including the liver². In this study, by using the human liver ductal organoids as
161 model, we have clearly shown that SARS-CoV-2 can infect the cholangiocytes and
162 impair their barrier and bile acid transporting functions. This could be due to the
163 direct viral cytopathogenic effect on target cells that express the ACE2 as entry
164 receptor. The viral infection may also down-regulate the expression of host genes
165 involved in the formation of tight junction and transportation of bile acid. Thus, it is
166 noteworthy to take into account the fact that the liver damage in COVID-19 patients
167 might be in part the result of direct cholangiocyte injury and consequent bile acid

168 accumulation caused by SARS-CoV-2 infection, which should be cautious in clinical

169 treatment.

170 By employing human liver ductal organoids, we have investigated the infection and

171 liver tissue damage of SARS-CoV-2 ex vivo. Besides the dissection of viral

172 pathogenesis, this platform could also be applied to evaluate the efficacy of novel

173 anti-viral drugs, especially when ideal animal models are lacking.

174

175 **Methods**

176 **Human biopsy.**

177 Human liver biopsies were obtained and used for research purposes with approval
178 from the Medical Ethical Council of Zhongshan Hospital. The study abides by the
179 Declaration of Helsinki principles.

180

181 **Virus stock preparation.**

182 SARS-CoV-2 was isolated from a COVID-19 patient in Shanghai, China
183 (SARS-CoV-2/SH01/human/2020/CHN, GenBank accession no. MT121215). Virus was
184 plaque-purified, propagated in Vero-E6 cells, and stored at -80°C for use. All
185 experiments involving virus infections were done in biosafety level 3 facility strictly
186 following the regulations.

187

188 **Liver ductal organoid culture and SARS-CoV-2 infection.**

189 The human ductal organoids were generated from primary bile ducts isolated
190 from human liver biopsies as described by Huch et al¹⁷. The organoids embedded in
191 Matrigel (Corning, 356231) were scrambled off the plate and collected in tubes, then
192 washed with cold PBS by pipetting the material up and down for 10 times. After
193 centrifugation (2 min at 250 g), the organoid pellet was suspended with medium
194 containing 5 μM Y-27632 (Sigma-Aldrich, Y0503). Around 200-300 organoids were
195 infected with 1.2×10^5 PFU of SARS-CoV-2 in 24 well plate containing 500 μL medium
196 and incubated at 37 $^{\circ}\text{C}$ for 1 hour. After incubation, organoids were collected by

197 pipetting and washed once with PBS, then repeated the centrifugation and removed
198 supernatant. The organoids were embedded with Matrigel, followed by seeding on a
199 24-well plate. After polymerization, culture medium was added.

200

201 **Immunofluorescence.**

202 For whole mounting liver organoids staining, organoids were fixed in 4%
203 paraformaldehyde for 30 min at 4 °C, washed with PBS and permeabilized with 0.25%
204 Triton X-100 (Sigma-Aldrich, X100) in PBS for 30 min. The organoids were then
205 washed with PBST (PBS containing 0.1% Tween 20) and blocked by 5% BSA in PBST
206 for 1 hour at room temperature. Organoids were incubated with the primary
207 antibodies at 4 °C overnight, washed with PBST 3 times, and incubated with the
208 secondary antibodies and DAPI for 1 hour at room temperature. Organoids imaging
209 was performed on confocal microscope (OLYMPUS, FV3000). The following
210 antibodies were used: rabbit anti-ACE2 (Sino Biological Inc, 10108-RP01, 1:100),
211 rabbit anti-SARS-CoV-2 N protein (Rockland, 200-401-A50, 1:500), mouse
212 anti-E-cadherin (BD Biosciences, 610181), Cy3-conjugated donkey anti-rabbit IgG
213 (Jackson Lab, 711-165-152), Alexa Fluor 488-conjugated donkey anti-mouse IgG
214 (Jackson Lab, 715-545-151).

215

216 **Quantitative RT-PCR.**

217 Total RNA was isolated from organoids by RNeasy Mini kit (QIAGEN,74106) and
218 reverse-transcribed into cDNA with M-MLV Reverse Transcriptase (Invitrogen,

219 28025013). Quantitative real-time PCR was performed on CFX384 Touch System (Bio
220 Rad). Primers used were listed in Table 1. The SARS-CoV-2 primer and probe sets
221 were provided by Integrated DNA Technologies (IDT, 10006606).

222

223 **Single-cell RNA seq and data analysis.**

224 Single-cell RNA sequencing was performed using the 10x Genomics Chromium
225 System. Human liver ductal tissues were derived from a patient who underwent
226 resection, cultured for 3 passages as described above. Mouse primary liver ductal
227 organoids were cultured from biliary ducts isolated from an 8-week-old C57BL/6
228 mouse. Briefly, organoids were dissociated with 1× TrypLE Select Enzyme (Gibco,
229 12563011) to obtain single cell suspension. A total of around 8,000 cells per sample
230 were captured on a 10×Chromium device and library preparation was carried out
231 using Single Cell 3' Reagent Kits v2 according to the manufacturer's instructions (10×
232 Genomics). Libraries were sequenced on an Illumina NovaSeq 6000 platform.

233 Cell Ranger (version 3.1) with default parameters was used to process sequencing
234 data to generate feature-barcode matrices. The human dataset was analyzed using
235 the standard workflow on the Seurat R Package (version 3.1.3) (Butler et al., 2018).
236 For the feature-barcode matrix of 8,094 cells from the human dataset, we removed
237 cells with less than 500 genes and more than 6,000 genes as well as cells with high
238 fraction of mitochondrial UMIs (> 20%). 7,978 high quality cells and 17,447
239 expressed genes were remained for downstream analysis. The cell populations were
240 clustered using the 'FindClusters' function and visualized in 2 dimensions by

241 t-distributed stochastic neighbor embedding (t-SNE) derived from the top 10
242 principal components. For the feature-barcode matrix of 9,690 cells from the mouse
243 dataset, we retained cells with expressed genes between 500 and 6,000 as well as
244 cells with low fraction of mitochondrial UMIs (< 10%). Finally, 8,812 high quality cells
245 and 16,019 expressed genes were remained for downstream analysis. The
246 integration of human and mouse datasets was processed by the standard Seurat v3
247 integration workflow.

248

249 **Statistical analysis.**

250 We employed Student's *t*-test or ANOVA test to analyze the parametric
251 experimental results. Significant differences were noted with asterisks.

252 **Acknowledgments**

253 The authors thank Dr. Stacey S. Huppert for technical assistance. We also wish to
254 acknowledge Di Qu, Xia Cai, Zhiping Sun, Wendong Han and the others at Biosafety
255 Level 3 Laboratory of Fudan University for experiment design and expert technical
256 assistance. This work was supported by grants from the National Key Research and
257 Development Program of China (2018YFA0109400 and 2018YFA0109800), the
258 Zhejiang University Special Scientific Research Fund for COVID-19 Prevention and
259 Control (2020XGZX013) and the Shanghai Municipal Science and Technology Major
260 Project (2017SHZDZX01). B.Z. was sponsored by Shanghai Rising-Star Program and
261 Eastern Scholar Program.

262

263 **Author Contributions**

264 B.Z., C.N. and R.Z. conceived the study; B.Z., C.N., R.G., Y.W., L.Y., J.W., T.L., J.L.,
265 W.X.,. and R.Z. performed the experiments; B.Z., J.L., R.Z. and X.L. supervised the
266 work; Y.X X.W. and Z.Y. contributed to the discussion of the results; and B.Z., C.N.,
267 R.Z. and X.L. wrote the manuscript.

268

269 **Conflict of interest**

270 The authors declare that they have no conflict of interest.

271

272 References

273

- 274 1 Wu, F. *et al.* A new coronavirus associated with human respiratory disease in China. *Nature*,
275 doi:10.1038/s41586-020-2008-3 (2020).
- 276 2 Huang, C. *et al.* Clinical features of patients infected with 2019 novel coronavirus in Wuhan,
277 China. *Lancet*, doi:10.1016/S0140-6736(20)30183-5 (2020).
- 278 3 Chen, N. *et al.* Epidemiological and clinical characteristics of 99 cases of 2019 novel
279 coronavirus pneumonia in Wuhan, China: a descriptive study. *Lancet*,
280 doi:10.1016/S0140-6736(20)30211-7 (2020).
- 281 4 Zhu, N. *et al.* A Novel Coronavirus from Patients with Pneumonia in China, 2019. *N Engl J Med*,
282 doi:10.1056/NEJMoa2001017 (2020).
- 283 5 Fan, Z. *et al.* Clinical Features of COVID-19 Related Liver Damage. *medRxiv* (2020).
- 284 6 Zhou, P. *et al.* A pneumonia outbreak associated with a new coronavirus of probable bat
285 origin. *Nature*, doi:10.1038/s41586-020-2012-7 (2020).
- 286 7 Wan, Y., Shang, J., Graham, R., Baric, R. S. & Li, F. Receptor recognition by novel coronavirus
287 from Wuhan: An analysis based on decade-long structural studies of SARS. *J Virol*,
288 doi:10.1128/JVI.00127-20 (2020).
- 289 8 Chen, Y., Guo, Y., Pan, Y. & Zhao, Z. J. Structure analysis of the receptor binding of 2019-nCoV.
290 *Biochem Biophys Res Commun*, doi:10.1016/j.bbrc.2020.02.071 (2020).
- 291 9 Kuhn, J. H., Li, W., Choe, H. & Farzan, M. Angiotensin-converting enzyme 2: a functional
292 receptor for SARS coronavirus. *Cell Mol Life Sci* **61**, 2738-2743,
293 doi:10.1007/s00018-004-4242-5 (2004).
- 294 10 Hoffmann, M. *et al.* SARS-CoV-2 Cell Entry Depends on ACE2 and TMPRSS2 and Is Blocked by
295 a Clinically Proven Protease Inhibitor. *Cell*, doi:10.1016/j.cell.2020.02.052 (2020).
- 296 11 Zhao, Y. *et al.* Single-cell RNA expression profiling of ACE2, the putative receptor of Wuhan
297 2019-nCoV. *bioRxiv*, doi:10.1101/2020.01.26.919985 (2020).
- 298 12 Zhang, H. *et al.* The digestive system is a potential route of 2019-nCoV infection: a
299 bioinformatics analysis based on single-cell transcriptomes. *bioRxiv* (2020).
- 300 13 Qi, F., Qian, S., Zhang, S. & Zhang, Z. Single cell RNA sequencing of 13 human tissues identify
301 cell types and receptors of human coronaviruses. *bioRxiv* (2020).
- 302 14 Chai, X. *et al.* Specific ACE2 Expression in Cholangiocytes May Cause Liver Damage After
303 2019-nCoV Infection. *bioRxiv* doi:10.1101/2020.02.03.931766 (2020).
- 304 15 Xu, Z. *et al.* Pathological findings of COVID-19 associated with acute respiratory distress
305 syndrome. *Lancet Respir Med*, doi:10.1016/S2213-2600(20)30076-X (2020).
- 306 16 Dutta, D. & Clevers, H. Organoid culture systems to study host-pathogen interactions. *Curr*
307 *Opin Immunol* **48**, 15-22, doi:10.1016/j.coi.2017.07.012 (2017).
- 308 17 Huch, M. *et al.* Long-term culture of genome-stable bipotent stem cells from adult human
309 liver. *Cell* **160**, 299-312, doi:10.1016/j.cell.2014.11.050 (2015).

310

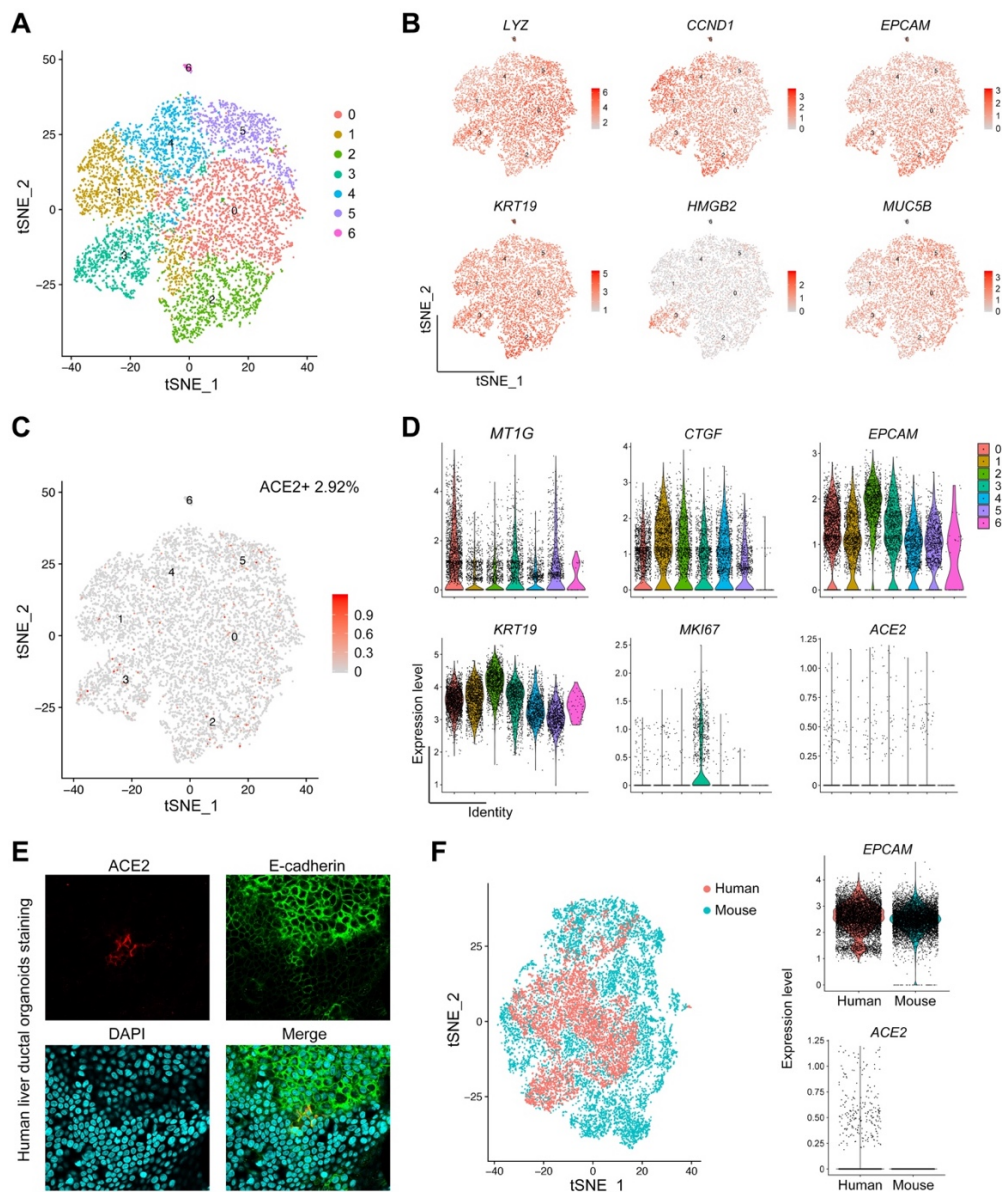
311

312

313

314

Figure 1



315

316 **Figure 1 | ACE2+ cholangiocytes are preserved in human liver ductal organoid**

317 **cultures.** (A) Cell-type clusters. t-SNE visualization of the cell populations

318 (color-coded for clusters) from human liver ductal organoids by t-SNE. (B) t-SNE

319 plots indicating the expression of representative marker genes. (C) t-SNE plots

320 indicating the expression of ACE2 gene. (D) Violin plots showing the expression of

321 representative marker genes. (E) Immunofluorescence staining for ACE2 and

322 E-cadherin in human liver ductal organoids. Results were representative of three

323 independent experiments. (F) t-SNE visualization of single cells isolated from human

324 and mouse liver ductal organoids; Violin plots showing the expression of EPCAM and

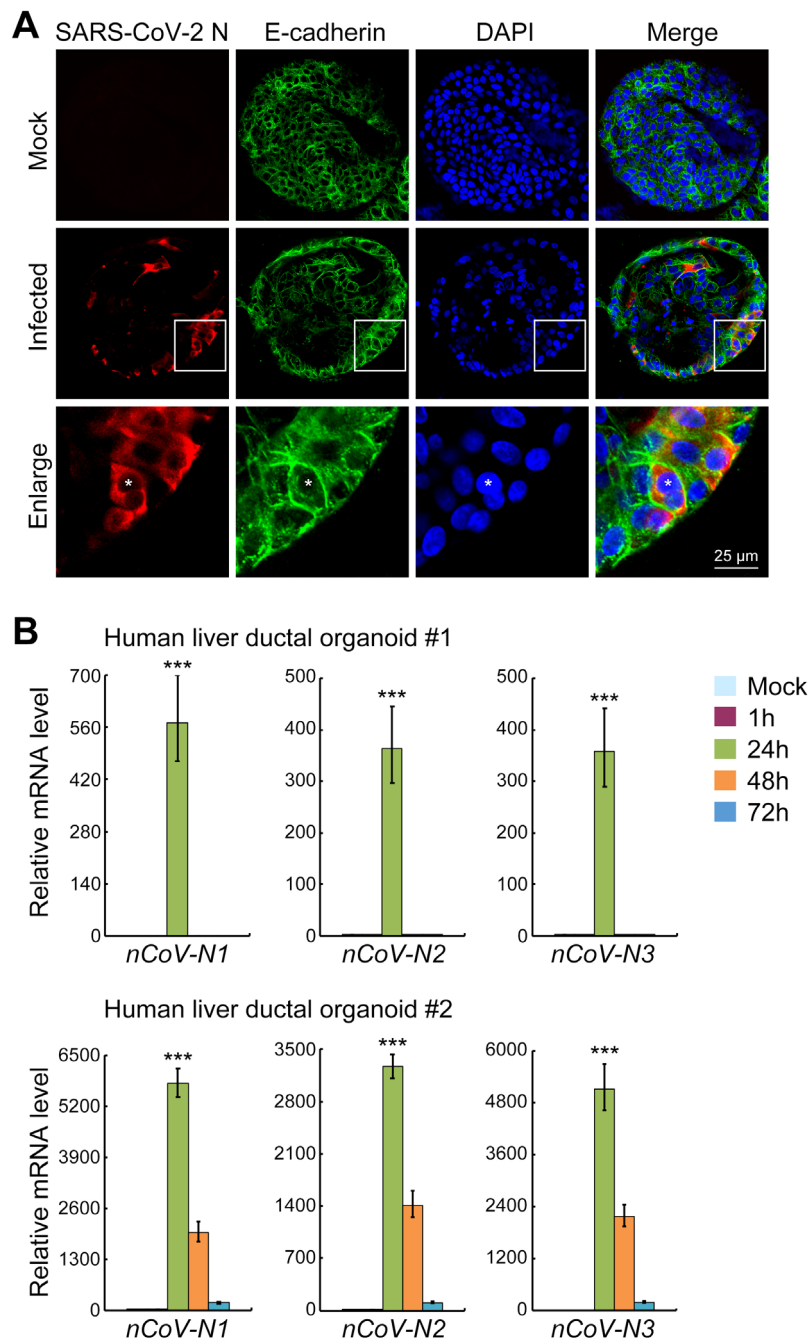
325 ACE2.

326

327

Figure 2

328



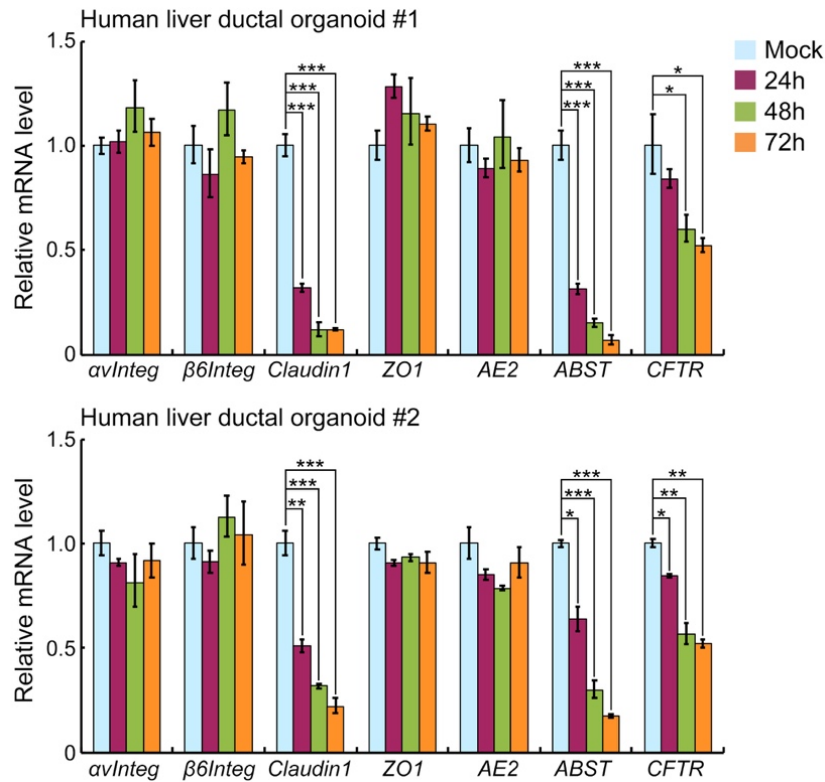
329

330 **Figure 2 | Recapitulation of SARS-CoV-2 infection in human Liver ductal**
331 **organoids.** (A) Immunofluorescence staining for SARS-CoV-2 N protein and
332 E-cadherin in human liver ductal organoids. (B) Two cases of human liver ductal
333 organoids were harvested at indicated time points following SARS-CoV-2 infection to
334 examine the virus load using qRT-PCR. *RNP* was used as an internal control. Data
335 were presented as mean±s.d. *** indicates $p < 0.001$.

336

Figure 3

337



338

339 **Figure 3 | SARS-CoV-2 infection impairs the barrier and bile acid transporting**

340 **functions of cholangiocytes.** Two cases of human liver ductal organoids after

341 SARS-CoV-2 infection were harvested to examine the expression of indicated genes

342 using qRT-PCR. *GAPDH* was used as an internal control. Data were presented as

343 mean±s.d. * indicates $p<0.05$; ** indicates $p<0.01$; *** indicates $p<0.001$.

344

345 **Table 1 | Primers and probes for qRT-PCR.**

346

TaqMan primers and probes	Oligonucleotide sequence (5'-3')
<i>nCov-N1</i> forward	GACCCCAAATCAGCGAAAT
<i>nCov-N1</i> reverse	TCTGGTTACTGCCAGTTGAATCTG
<i>nCov-N1</i> probe	FAM-ACCCCGCATTACGTTTGGTGGACC-BHQ1
<i>nCov-N2</i> forward	TTACAAACATTGGCCGCAA
<i>nCov-N2</i> reverse	GCGCGACATTCCGAAGAA
<i>nCov-N2</i> probe	FAM-ACAATTTGCCCCAGCGCTTCAG-BHQ1
<i>nCov-N3</i> forward	GGGAGCCTTGAATACACCAAAA
<i>nCov-N3</i> reverse	TGTAGCACGATTGCAGCATTG
<i>nCov-N3</i> probe	FAM-AYCACATTGGCACCCGCAATCCTG-BHQ1
<i>RNP</i> forward	AGATTTGGACCTGCGAGCG
<i>RNP</i> reverse	GAGCGGCTGTCTCCACAAGT
<i>RNP</i> probe	FAM-TTCTGACCTGAAGGCTCTGCGCG-BHQ1

347

qRT-PCR primers	Forward (5'-3')	Reverse (5'-3')
<i>ACE2</i>	CATTGGAGCAAGTGTGGATCTT	GAGCTAATGCATGCCATTCTCA
<i>GAPDH</i>	GGTATCGTGGAAGGACTCATGAC	ATGCCAGTGAGCTTCCCCTTCAG
<i>av integrin</i>	GGGATGACAACCCTCTGAC	GTTTCTCAGCTCATAGATGTG
<i>β6 integrin</i>	CTGCTTTGCCTGTTCTTTCTATTTC	GTTTCTGCACCTCCCAGGG
<i>Claudin-1</i>	GTGCGATATTTCTTCTTGCAAGTC	TTCGTACCTGGCATTGACTGG
<i>JAM-A</i>	GCGCAAGTCGAGAGGAAACT	AAAAGCCCGAGTAGGCACAG
<i>Claudin-4</i>	GGCTGCTTTGCTGCAACTGTC	GAGCCGTGGCACCTTACACG
<i>ZO-1</i>	GTGTTGTGGATACCTTGT	GATGATGCCTCGTTCTAC
<i>Muc2</i>	GCGATGCCTACACCAAAGT	TGATCTTCTGCATGTTCCCA
<i>Muc5ac</i>	GGACCAAGTGGTTTGACACTGAC	CCTCATAGTTGAGGCACATCCCAG
<i>EP4</i>	GACCTGTTGGGCACTTTGTT	TGGACGCATAGACTGCAAAG
<i>CFTR</i>	TGACCTTCTGCCTCTTACCA	CACTATCACTGGCACTGTTGC
<i>AE2</i>	TCCTCCCACCACATCCATCA	CTCCTCAATGGTCGGGGTTTC
<i>ABST</i>	CAGTTTGGAAATCATGCCCTC	GCTATGAGCACAATGAGGATGG

348